

# Analysis of the influence of the stochastic variability of the raindrop size distribution on radar attenuation correction

A. Berne and R. Uijlenhoet

Hydrology and Quantitative Water Management Group, Wageningen University, The Netherlands

**Abstract.** To analyze the influence of the stochastic nature of the drop size distribution (DSD) and the influence of the rainfall heterogeneity on the robustness and the accuracy of attenuation correction algorithms, a stochastic model has been developed to simulate profiles of DSD and consequently profiles of rainfall intensity, radar reflectivity and specific attenuation. Using a Monte Carlo technique, it is shown that an attenuation correction algorithm based on a forward implementation is more sensitive to the inadequacy of power-law relations and to heterogeneity than a backward algorithm. For both types, the corrected profiles remains uncertain, because of the stochastic nature of the raindrop size distribution.

## 1 Introduction

Hydrological applications such as flood forecasting and risk management require quantitative precipitation estimates. To obtain robust and accurate rainfall estimates using weather radar, the conversion between the radar reflectivity factor  $Z$  (in  $\text{mm}^6 \text{m}^{-3}$ ) and the rainfall intensity  $R$  (in  $\text{mm h}^{-1}$ ) is a crucial step. Moreover, the importance of attenuation affecting the radar signal in rain has been recognized for a long time in the case of C- or X-band wavelengths (e.g. Atlas and Banks, 1951; Hitschfeld and Bordan, 1954). With the launch of airborne and spaceborne radars, various techniques have been developed to correct for the attenuation due to rainfall. They can be separated into two categories: the algorithms which start at the radar and propagate with increasing range (forward algorithms); and those which start at a given range and propagate toward the radar (backward algorithms). All these algorithms are based on power law relations between the integrated radar variables  $Z$ ,  $R$  and  $k$ , the one-way specific attenuation (in  $\text{dB km}^{-1}$ ), which are weighted statistical moments of the raindrop size distribution (DSD here-

after). These power laws have first been empirically established (e.g. Marshall and Palmer, 1948). Sempere-Torres et al. (1994) introduced the generalized DSD framework, based on the normalization of the DSD by a single moment. It is then possible to show that this scaling formalism for the DSD results in power-law relations between the integrated variables. Recently, Lee et al. (2004) proposed a double-moment normalization framework in order to describe more completely the DSD. However all these approaches are based on deterministic relations between stochastic variables. The main objectives of this paper are to investigate for the attenuation correction (1) the adequacy of such deterministic power-law relations between  $Z$ ,  $k$ ,  $R$ ; and (2) the uncertainty due to the rainfall heterogeneity within the radar resolution volume, also called non-uniform beam filling. In particular we shall focus on a forward algorithm derived from the analytical solution proposed by Hitschfeld and Bordan (1954), and a backward algorithm derived from the solution proposed by Marzoug and Amayenc (1994).

We choose to use a simulation framework for this study in order to control the different processes involved. Hence we need to produce profiles (in space) of DSDs which allow to derive all the variables of interest ( $R$ ,  $Z$  and  $k$ ). The method used to produce these DSD profiles is described in Sect. 2. The algorithms applied for attenuation correction are discussed in Sect. 3. An analysis of the performance of the two algorithms is presented in Sect. 4. Finally, Sect. 5 provides the conclusions.

## 2 DSD profiles simulation

We want to simulate DSDs in space with realistic features. The first step consists of the development of a stochastic DSD model. Then its parameters must be deduced from DSD measurement to generate realistic profiles. A first step will be to fix a statistical law for the DSD and then to produce profiles. In order to have realistic correlation characteristics

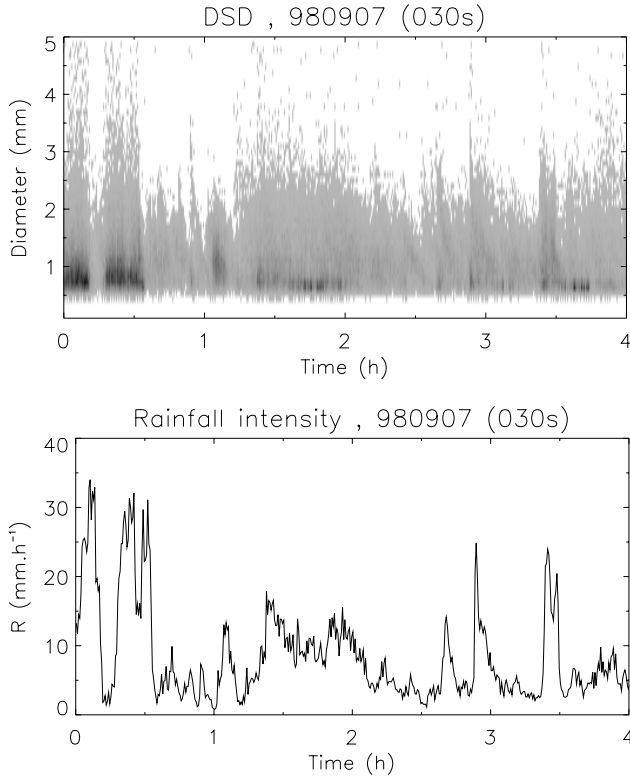


**Fig. 1.** DSD spectra (number of drops) and rainfall intensity ( $\text{mm h}^{-1}$ ) for the considered 4 h rainy period.

within the profiles, their simulation will be constrained by DSD measurements.

## 2.1 Formulation

To keep the formulation simple and the computation time reasonable, we choose an exponential law for the DSD:

$$N(D) = \frac{N_t}{D_m} e^{-\frac{D}{D_m}} \quad (1)$$

where  $D$  is the diameter,  $N(D)dD$  represents the number of drops of diameter between  $D$  and  $D + dD$ ,  $N_t$  is the concentration of drops per unit volume and  $D_m$  is the mean diameter. Assuming  $N_t$  and  $D_m$  follow a bivariate lognormal distribution (Smith and De Veaux, 1994) and defining  $N' = \ln N_t$  and  $D' = \ln D_m$ , yields for the joint probability density function (pdf):

$$f(N', D') = \mathcal{N}(\mu_{N'}, \mu_{D'}, \sigma_{N'}, \sigma_{D'}, \rho_{N'D'}) \quad (2)$$

where  $\mathcal{N}$  denotes the bivariate normal distribution,  $\mu_{N'}$  represents the mean of  $N'$ ,  $\sigma_{N'}$  its standard deviation (the same notation is used for  $D'$ ) and  $\rho_{N'D'}$  represents the correlation between  $N'$  and  $D'$ . We are now able to simulate the DSD at one point. This realization is used as the starting point to generate the DSD profile. We assume that it can be described

as a discrete stationary vector auto-regressive (VAR) process of order 1:

$$\mathbf{X}[k+1] = \mathbf{C}_1 \mathbf{C}_0^{-1} \mathbf{X}[k] + \mathbf{E}[k+1] \quad (3)$$

where

$$\begin{aligned} \mathbf{X}[k] &= \begin{bmatrix} N'(k) - \mu_{N'} \\ D'(k) - \mu_{D'} \end{bmatrix} \\ \mathbf{C}_0 &= \begin{bmatrix} \sigma_{N'}^2 & \sigma_{N'}\sigma_{D'}\rho_{N'D'} \\ \sigma_{N'}\sigma_{D'}\rho_{N'D'} & \sigma_{D'}^2 \end{bmatrix} \\ \mathbf{C}_1 &= \begin{bmatrix} \sigma_{N'}^2\rho_{N'}(1) & \sigma_{N'}\sigma_{D'}\rho_{N'D'}(1) \\ \sigma_{N'}\sigma_{D'}\rho_{D'N'}(1) & \sigma_{D'}^2\rho_{D'}(1) \end{bmatrix} \\ \mathbf{E}[k+1] &= \begin{bmatrix} \epsilon_{N'}(k+1) \\ \epsilon_{D'}(k+1) \end{bmatrix} \end{aligned}$$

$k$  is the distance index,  $\rho_{N'D'}(1)$  represents the cross-correlation at the distance lag 1,  $\rho_{N'}(1)$  represents the auto-correlation at lag 1 (idem for  $D'$ ) and  $\epsilon_{N'}$  represents a white noise process (idem for  $D'$ ). Therefore  $\mathbf{C}_0$  and  $\mathbf{C}_1$  are the covariance matrices at the lags 0 and 1. The variances of the white noise processes  $\epsilon_{N'}$  and  $\epsilon_{D'}$  are fixed so that  $\mathbf{X}$  is a second order stationary process. It must be noted that the auto-correlation function of a first order VAR is exponential:

$$\rho(k\Delta r) = e^{ak\Delta r} \quad (4)$$

where  $\Delta r$  represents the spatial resolution.

Once the DSD profile is generated, we can deduce the corresponding profiles of the integrated variables  $R$ ,  $Z$  and  $k$ . We use the model proposed by Beard (1976) for the raindrop terminal fall speed and the Mie theory for the backscattering and extinction coefficients.

## 2.2 Parameterization

The statistical model described above has 9 parameters: 5 for the lognormal distribution ( $\mu_{N'}$ ,  $\sigma_{N'}$ ,  $\mu_{D'}$ ,  $\sigma_{D'}$  and  $\rho_{N'D'}$ ) and 4 for the VAR process ( $\rho_{N'}(1)$ ,  $\rho_{D'}(1)$ ,  $\rho_{N'D'}(1)$  and  $\rho_{D'N'}(1)$ ).

Let us first focus on the estimation of the parameters for the lognormal distribution. During the HIRE98 experiment (Uijlenhoet et al., 1999), DSD measurements have been performed using two optical spectropluviometers. They provide the opportunity to estimate the statistical characteristics of  $N'$  and  $D'$  we need to run our DSD model. As we are interested in the attenuation of the radar signal due to rain, we select a 4 h period during an intense rain event, for which the path integrated attenuation (PIA hereafter) reached 30 dB. The measured DSDs and rainfall intensities are displayed in Fig. 1.

The parameters  $N_t$  and  $D_m$  of an exponential law are fitted to the measured diameter spectra, using the third (water content) and sixth (radar reflectivity) order moments (Waldvogel, 1974). The time series have a 30 s time step in order to have robust estimates and at the same in a not too coarse temporal integration. The obtained time series of  $N_t$  and  $D_m$  allow to estimate  $\mu_{N'}$ ,  $\sigma_{N'}$ ,  $\mu_{D'}$  and  $\sigma_{D'}$  (see Table 1).

**Table 1.** Mean and standard deviation of  $N$  (number of drops per  $\text{m}^{-3}$ ),  $D_m$  (in mm),  $N' = \ln N_t$  and  $D' = \ln D_m$  deduced from HIRE98 data.

Variable	$N_t$	$D_m$	$N'$	$D'$
Mean	20000	0.37	9.68	-1.03
Std	15000	0.1	0.45	0.07

We must now estimate the correlation parameters. Unfortunately, the time series of DSD measurements do not allow to derive the spatial auto- and cross-correlation for  $N'$  and  $D'$ . We reduce the number of correlation parameters assuming:

- $C_1$  is symmetric

$$\rho_{N'D'}(1) = \rho_{D'N'}(1)$$

- $N'$  and  $D'$  have the same auto-correlation function

$$\rho_{N'}(1) = \rho_{D'}(1)$$

- the cross-correlation follows the same exponential law as the auto-correlation (see Eq.4)

$$\rho_{N'D'}((k+1)\Delta r) = e^{\alpha\Delta r} \rho_{N'D'}(k\Delta r)$$

To estimate  $\alpha$ , we use the decorrelation distance of  $R$  which has been evaluated in a previous study of the same rain event (Berne et al., 2004). We assume that this decorrelation distance  $d = 5$  km is valid for  $N'$  and  $D'$ . As an exponential decorrelation function never reaches 0, we have to fix a threshold at which we consider the correlation is 0. Choosing 0.001 yields

$$\alpha = \frac{\ln 1000}{d} = 1.4 \times 10^{-3} (\text{m}^{-1}) \quad (5)$$

Finally the only remaining correlation parameter is  $\rho_{N'D'}$ . To avoid producing two very correlated ( $\rho_{N'D'} \sim 1$ ) or independent ( $\rho_{N'D'} \sim 0$ ) variables, we arbitrarily fix it at 0.5.

The model being parameterized, we have to choose the radar wavelength, the spatial resolution and the range to be simulated. As the attenuation effects are more important for X-band wavelengths, we select 3.2 cm as wavelength and the corresponding Mie coefficients have been calculated. To be able to study the influence of non-uniform beam filling, we choose to simulate high spatial resolution (10 m) profiles with a moderate range of 20 km. Figure 2 presents as example profiles of rainfall intensity  $R$ , reflectivity factor  $Z$  and the corresponding attenuated reflectivity factor  $Z_a$ .

### 3 Attenuation correction algorithms

As mentioned in the introduction, we shall use two different algorithms to analyze the influence of the stochastic variability

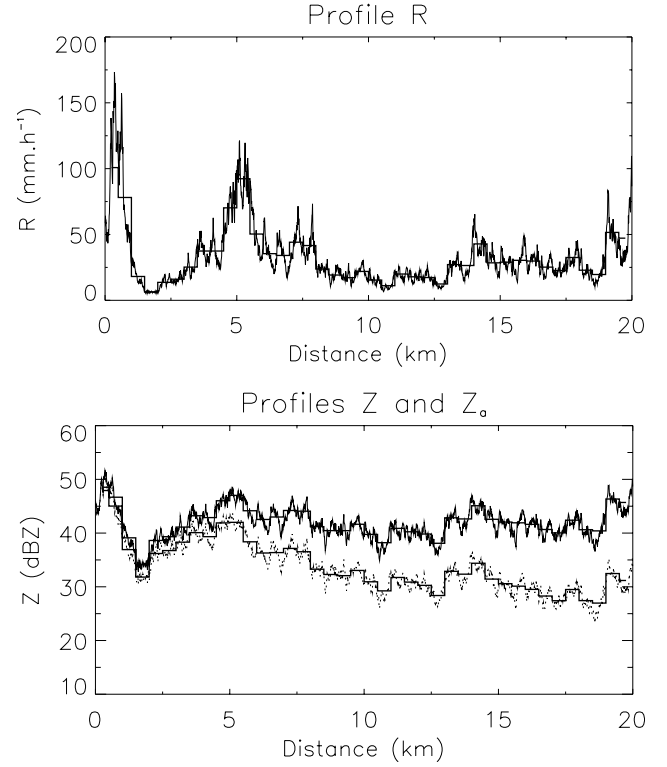


**Fig. 2.** Example of a profile of  $R$ ,  $Z$  and  $Z_a$  generated by the DSD model. The corresponding average profiles (over 500 m) are also displayed.

ity of the DSD. Assuming  $Z = c k^d$ , we have

$$Z_a(r) = Z(r) A(r)$$

$$A(r) = \exp \left[ -0.2 \ln(10) \int_0^r \left( \frac{Z(s)}{c} \right)^{1/d} ds \right] \quad (6)$$

where  $A(r)$  is the attenuation factor at the range  $r$  ( $A \in [0, 1]$ ). Hirschfeld and Bordan (1954) proposed an analytical solution to express  $A$  as a function of  $Z_a$ :

$$Z(r) = \frac{Z_a(r)}{\left[ 1 - \frac{0.2 \ln(10)}{d} \int_0^r (Z_a(s)/c)^{1/d} ds \right]^d} \quad (7)$$

The HB algorithm will designate this analytical solution applied to a discrete profile of  $Z_a$ . The HB algorithm is a forward algorithm because the integral is between 0 and  $r$ . However, the difference in its denominator can be close to 0 and makes the algorithm unstable (Delrieu et al., 1999).

To avoid instability problems, another family of attenuation correction algorithms has been developed. It is based on the knowledge of the PIA at a given range  $r_0$ . The reformulation of Eq. (7) starting from  $r_0$  and going backward to the radar guarantees the stability of the algorithms. As example, we use the solution (and the corresponding algorithm) proposed by Marzoug and Amayenc (1994):

$$Z(r) = \frac{Z_a(r)}{\left[ A(r_0)^{1/d} + \frac{0.2 \ln(10)}{d} \int_r^{r_0} (Z_a(s)/c)^{1/d} ds \right]^d} \quad (8)$$

**Table 2.** Prefactors ( $a$  and  $c$ ) and exponents ( $b$  and  $d$ ) of the climatological  $Z = a R^b$  and  $Z = c k^d$  relations. Mean, standard deviation and coefficient of variation of the prefactors and exponents from the same relations derived from the 1000 profiles.

	$a$	$b$	$c$	$d$
Climatology	237	1.26	60073	1.16
Mean	232	1.27	59328	1.14
Std	67	0.08	1187	0.03
CV	0.29	0.06	0.02	0.03

The main drawback of such a backward algorithm is that it requires a reliable estimation of the PIA at a given range. The DSD is a random function and so are its statistical moments  $R$  and  $Z$ . The objective of this paper is to investigate the consistency between the deterministic power-law relations used in the attenuation correction algorithms and the stochastic nature of the variables. To study the robustness and the accuracy of the algorithms, we propose to use a Monte Carlo technique. First, 1000 independent triplets ( $Z$ ,  $k$ ,  $R$ ) are generated and a set of power-law relations ( $Z$ – $R$  and  $Z$ – $k$ ) is fitted using a non-linear optimization technique. They are designated as the climatological relations. Second, 1000 profiles of  $R$ ,  $Z$  and  $k$  (hence  $Z_a$ ) are generated. On each profile a power-law relation set is fitted separately. It must be noted that they constitute the best possible relations. To study the non-uniform beam filling, the high spatial resolution (10 m) profiles are averaged at a lower spatial resolution (500 m). Then the two algorithms are applied using the best and the climatological relations on the 1000 high and low resolution profiles. The corrected  $Z$  profiles converted to rainfall intensity are designated as the corrected  $R$  profiles. The root mean square error (RMSE) calculated between the true and the corrected  $R$  profiles is used as quality criterion, because it can be averaged over the number of profiles.

## 4 Results

First, we can compare the climatological power-law relations and the statistics of the relations derived from the 1000 profiles (see Table 2).

The climatological and mean values are very close. But the variations of the prefactors and the exponents are significant and illustrate that the same DSD can result in different power-law relations. The non-linearity of the  $Z$ – $k$  relation is less strong because the exponent is closer to 1. Hence the relative dispersion of the prefactor and the exponent values is larger for the  $Z$ – $R$  relation, as indicated by the larger values of the coefficient of variation.

Figure 3 presents the RMSE values for 4 configurations (best-climatological relations and high-low resolution).

It clearly shows that the MA algorithm is more robust and accurate than the HB algorithm (if the PIA is known exactly).

Moreover, the two algorithms exhibit different behaviours. The scatter of the RSME values for the HB algorithm is more important than for the MA algorithm, for the 4 configurations. When the HB algorithm diverges, the RMSE is limited to  $10^4$ . The number of diverging profiles is larger for the low resolution profiles (about 350) than for the high resolution profiles (about 250).

It must be noted that no algorithm is able to achieve a perfect correction despite using the best power-law relations and the exact high resolution  $Z$  profiles. For the MA algorithm, the error remains small but is still significant: about  $2 \text{ mm h}^{-1}$  for a PIA of 15 dB and about  $8 \text{ mm h}^{-1}$  for a PIA of 30 dB. The complementary information provided by the knowledge of the PIA is not sufficient to completely correct for the attenuation. This deviation from the true rainfall profiles comes only from the fact that the relations between  $Z$ ,  $R$  and  $k$  are not exactly power-law relations. The error increases when the PIA increases and when a spatial averaging is performed (see graphs 3 and 4 of Fig. 3). The last graph corresponds to radar measurements, as a combination of spatial averaging and climatological relations. The minimum error for moderate PIA (15 dB) is larger than  $10 \text{ mm h}^{-1}$  and increases with the PIA. It shows the strong impact of non-uniform beam filling on attenuation correction.

## 5 Conclusions

A stochastic model has been developed to simulate realistic spatial profiles of DSD. It is based on an exponential DSD which two parameters follow a bivariate lognormal distribution. DSD measurements from the HIRE98 experiment have been used to parameterize the lognormal distribution. The profiles are produced by means of a first order vector autoregressive process with given correlation characteristics. It is important to underline that the different profiles generated by the model are different realizations of only one DSD.

From these DSD profiles, it is possible to derive the profiles of the variables which are of interest for radar rainfall estimation, i.e. the rainfall intensity  $R$ , the radar reflectivity factor  $Z$  and the specific one-way attenuation  $k$ . Thus a controlled experiment framework has been built to analyze the influence of the stochastic nature of the DSD on the attenuation correction. Focusing on X-band wavelengths, we used a Monte Carlo technique to study the robustness and the accuracy of two different attenuation correction algorithms. The first one (HB algorithm) corresponds to a forward implementation and is known for its instability. The second one (MA algorithm) corresponds to a backward implementation and is stable, but requires an additional information which is the PIA at a certain range from the radar.

The adequacy of power-law relations between the variables of interest as well as the effect of non-uniform beam filling have been investigated. The non-perfect fit of the power-law relations induces errors, in particular for large PIA, which are small but still significant for the MA algorithm, and which can become huge for the HB algorithm.

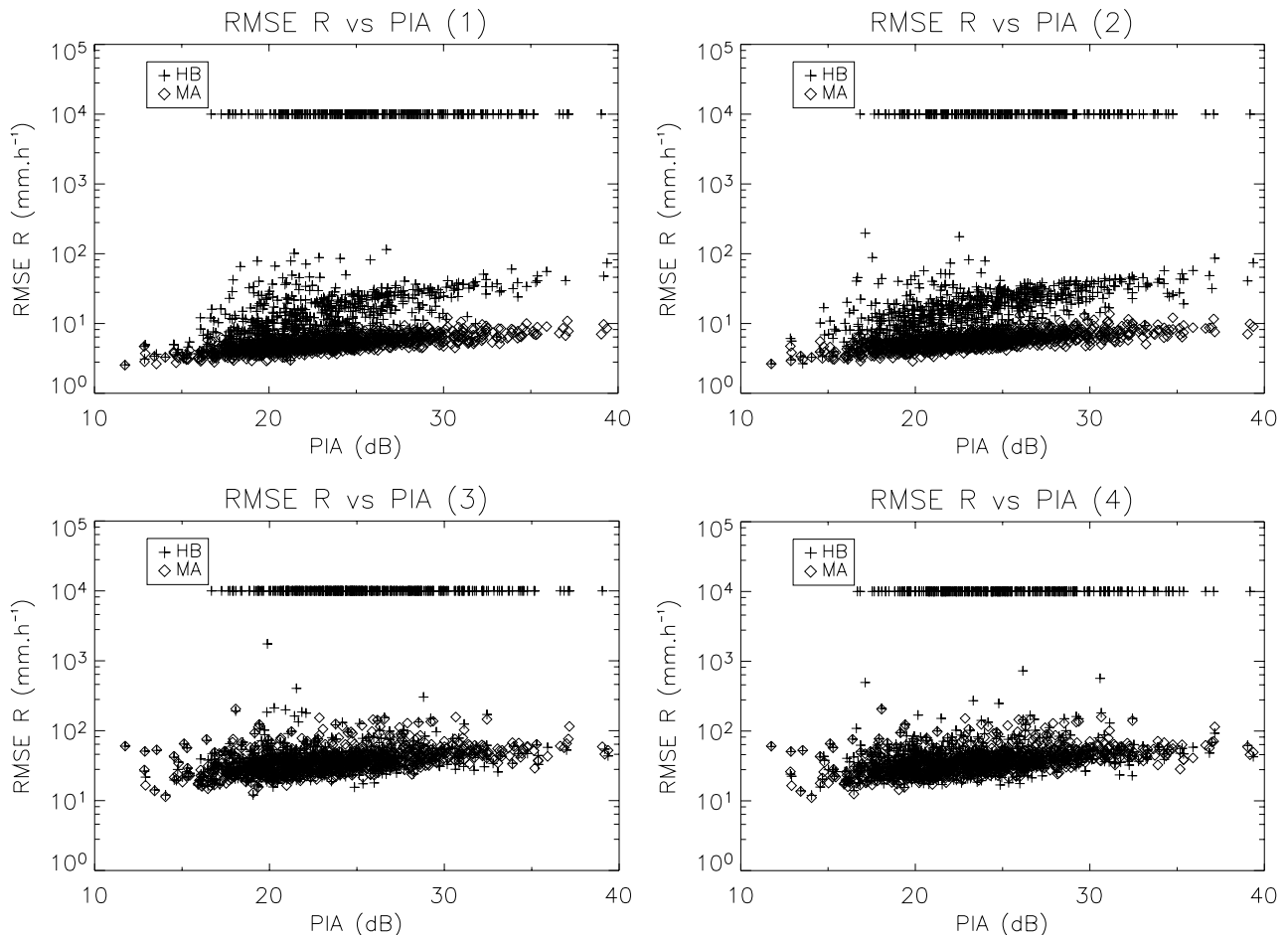


**Fig. 3.** RMSE for the HB and MA algorithms, for the 4 studied configurations: (1) high resolution – best relations; (2) high resolution – climatological relations; (3) low resolution – best relations; and (4) low resolution – climatological relations.

The non-uniform beam filling, studied by means of spatial averaging, significantly increases the error for both algorithms.

Further research is needed to study different types of precipitation and also to extend this work to C-band which is widely used in operational radar networks. Furthermore, the DSD simulation model offers opportunities to investigate the influence of various sources of error (e.g. calibration error, PIA uncertainty) and the question of the sampling error on DSD measurements.

**Acknowledgements.** The first author acknowledges financial support from the European Commission through a Marie Curie Post-doctoral Fellowship (Grant EVK1-CT-2002-50016). The second author is supported by the Netherlands Organization for Scientific Research (NWO) through Grant 016.021.003. This research is also supported by the European Commission through the FP6 Integrated Project FLOODsite.

## References

- Atlas, D. and Banks, H.: The interpretation of microwave reflections from rainfall, *J. Meteor.*, 8, 271–282, 1951.
- Beard, K.: Terminal velocity of cloud and precipitation drops aloft, *J. Atmos. Sci.*, 33, 851–864, 1976.
- Berne, A., Delrieu, G., Creutin, J.-D., and Obled, C.: Temporal and spatial resolution of rainfall measurements required for urban hydrology, *J. Hydrol.*, in press, 2004.
- Delrieu, G., Huckle, L., and Creutin, J.: Attenuation in rain for X-band and C-band weather radar systems : sensitivity with respect to the drop size distribution, *J. Appl. Meteor.*, 38, 57–68, 1999.
- Hitschfeld, W. and Bordan, J.: Errors inherent in the radar measurements of rainfall at attenuating wavelengths, *J. Meteor.*, 11, 58–67, 1954.
- Lee, G. W., Zawadzki, I., Szyrmer, W., Sempere-Torres, D., and Uijlenhoet, R.: A general approach to double-moment normalization of drop size distributions, *J. Appl. Meteor.*, 43, 264–281, 2004.
- Marshall, J. and Palmer, W.: The distribution of raindrops with size, *J. Meteor.*, 4, 186–192, 1948.
- Marzoug, M. and Amayenc, P.: A class of single and dual frequency algorithms for rain-rate profiling from a space born radar. Part I : principle and tests from numerical simulations, *J. Atmos.*

- Oceanic Technol., 11, 1480–1506, 1994.
- Sempere-Torres, D., Porrà, J., and Creutin, J.: A general formulation for raindrop size distribution, *J. Appl. Meteor.*, 33, 1494–1502, 1994.
- Smith, J. and De Veaux, R.: A stochastic model relating rainfall intensity to raindrop processes, *Water Resour. Res.*, 30, 651–664, 1994.
- Uijlenhoet, R., Andrieu, H., Austin, G., Baltas, E., Borga, M., Brilly, M., Cluckie, I., Creutin, J., Delrieu, G., Deshons, P., Fattorelli, S., Griffith, R., Guarnieri, P., Hang, D., Mimikou, M., Moani, M., Porrà, J., Sempere-torres, D., and Spagni, D.: HYDROMET Integrated Radar Experiment (HIRE) : experimental setup and first results, in 29th Int. Conf. On Radar Meteorology, AMS, pp. 926–930, Montreal, Canada, 1999.
- Waldvogel, A.: The  $N_0$  jump of raindrop spectra, *J. Atmos. Sci.*, 31, 1067–1078, 1974.